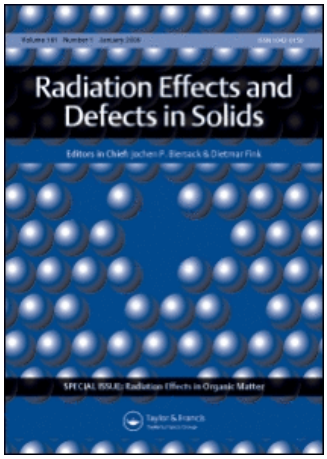

Radiation Effects and Defects in Solids
Publication details, including instructions for authors and subscription information:
http://www.informaworld.com/smpp/title~content=t713648881

UV-Laser irradiation effects on silver nanostructures

Online Publication Date: 01 July 2007
To cite this Article: Haro-Poniatowski, E., Batina, N., Acosta-García, M. C., Pohl-Alfaro, M. A., Castillo-Ocampo, P., Ricolleau, C. and Fort, E. (2007) 'UV-Laser irradiation effects on silver nanostructures', Radiation Effects and Defects in Solids, 162:7, 491 - 499
To link to this article: DOI: 10.1080/10420150701472213
URL: http://dx.doi.org/10.1080/10420150701472213

Radiation Effects & Defects in Solids
Vol. 162, Nos. 7–8, July–August 2007, 491–499

Taylor & Francis
Taylor & Francis Group

UV-Laser irradiation effects on silver nanostructures

E. HARO-PONIATOWSKI*†, N. BATINA‡, M. C. ACOSTA-GARCÍA‡,
M. A. POHL-ALFARO§, P. CASTILLO-OCAMPO¶, C. RICOLLEAU||, E. FORT||

†Departamento de Física,
‡Departamento de Química,
§Departamento de Ingeniería Eléctrica,
¶Laboratorio de Microscopía Electrónica, Universidad Autónoma Metropolitana Iztapalapa,
Av. San Rafael Atlixco No. 186 Col. Vicentina, C. P. 09340 México D. F., Mexico
||Laboratoire Matériaux et Phénomènes Quantiques and Laboratoire de Physique du
Solide, UMR 7162, CNRS/Université Paris 7–Denis Diderot, ESPCI, 10 rue Vauquelin,
75005 Paris Cedex, France

(Received 6 April 2007; revised 20 April 2007; in final form 23 April 2007)

The induced changes on silver nanostructures are investigated using a special experimental procedure consisting in depositing and subsequently inducing the changes directly on transmission electron microscopy grids. The nanostructures have different morphologies, from isolated spherical-like particles to quasi-percolated films. The UV laser-induced modifications were investigated using transmission electron microscopy and atomic force microscopy obtaining three-dimensional information on the nanostructures. Upon irradiation with a single laser pulse a quasi-percolated film is transformed into an assembly of silver nanoparticles. Upon further irradiation the nanoparticles grow in size. Furthermore the arrangement of these silver nanoparticles assemblies can be controlled by irradiating the nanostructured silver film through a mask. In the present work, we have used a transmission electron microscopy square grid as a diffractive device and have observed that the corresponding near field diffraction pattern is imprinted on the silver nanostructured film.

Keywords: Laser ablation; Silver nanoparticles; Laser irradiation; Patterning; AFM; TEM

1. Introduction

The optical properties of noble metal nanoparticles are strongly related to their size and shape. Depending on the desired application these nanoparticles are deposited on a surface, embedded in a matrix, or in solution. A fundamental issue has been the control of their size and shape. One possibility of manipulation of both characteristics is to use laser irradiation [1]. When the system is a solution the size of the nanoparticles decreases through a laser ablation mechanism [2]. These experiments have been performed in the nanosecond and femtosecond regimes [3–7]. In the case of embedded nanostructures silica-gel films containing Au nanoparticles have been fabricated by a photoreduction method. This system has been

*Corresponding author. Email: haro@xanum.uam.mx

Radiation Effects & Defects in Solids
ISSN 1042-0150 print/ISSN 1029-4953 online © 2007 Taylor & Francis
http://www.tandf.co.uk/journals
DOI: 10.1080/10420150701472213

proposed as a high-density optical recording medium [8]. By using two irradiation wavelengths a size reduction and a high-size uniformity of Ag nanoparticles on substrate surfaces have been obtained [9]. However, a size increase of the irradiated nanoparticles has also been observed [10, 11].

The change of shape and size has a dramatic effect on the surface plasmon properties of the nanoparticles. Surface plasmons of nanosized noble metals in colloidal suspensions or supported in thin films have been the object of detailed investigations [12, 13]. The case of embedded nanostructures in different solid matrices has also been considered. The particular interest in this field lies in the potential applications of these systems in surface enhanced spectroscopies such as Raman or fluorescence of biological molecules [14]. These nanostructured noble metals have been recently classified as 'plasmonic' materials and can be applied in the field of sensitive photonic devices to control, manipulate and amplify light on the nanometer length scale [15].

Another fundamental issue is the ordering of an ensemble of nanoparticles. This has been achieved using different techniques [11, 16].

In this work, we show first how to produce by laser irradiation a population of Ag nanoparticles with low dispersion in size distribution starting from a quasi-percolated Ag film. The Atomic Force Microscopy (AFM) characterization gives three-dimensional information, which is essential for understanding the photo-transformation processes involved upon laser irradiation. Secondly, starting with the same quasi-percolated film and using a diffractive mask we show how to obtain an ordered pattern of silver nanoparticles.

2. Preparation of the samples

The UHV chamber used in the synthesis of the nanoparticles has the capability of pulsed laser deposition (PLD) and classical thermal evaporation (TE). A typical target substrate configuration is used to deposit the alumina (Al_2O_3) by PLD using a KrF excimer laser at 248 nm with a pulse duration of 25 ns at a repetition rate of 4 Hz. The laser energy was of the order of 150 mJ. The distance from target to substrate was approximately 5 cm. The silver nanoparticles are deposited by TE at a pressure close to 10^{-8} mbar during evaporation. The source was a Knudsen type cell containing high purity Ag pellets heated at 1000 °C.

The substrates used were commercial transmission electron microscopy (TEM) grids prepared with an amorphous carbon layer. On the top of the amorphous carbon film a 3 nm layer of amorphous Al_2O_3 was deposited. The typical deposition rate was 1 nm/min. The silver amount deposited onto the alumina layer is equivalent to a layer thickness ranging from 3 nm to 50 nm of pure Ag metal. For short deposition times one obtains individual silver nanoparticles and as the deposition time increases different morphologies are obtained. From spherical to bean shape nanostructures. These bean shape nanostructures eventually coalesce to form 'fingered structures' that can be identified to a quasi-percolated film. In the experiments described in the present work such a quasi-percolated film was used. For longer deposition times a continuous film is obtained.

The same laser used for the PLD deposition process, is employed to irradiate the nanostructured samples. A focussing lens is placed in the laser beam to control the energy density. The experimental setup is shown in figure 1. The sample can be irradiated directly or through a diffractive device such as a second hollow (2000 mesh) TEM grid in the present case. Since the samples are prepared on TEM grids, they can be immediately observed by electron microscopy after irradiation.

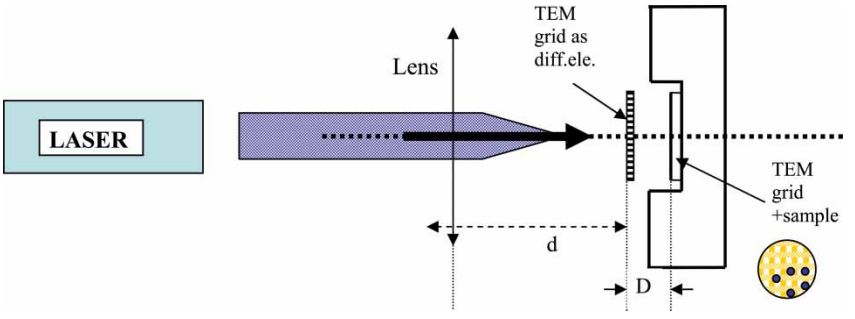

Figure 1. Experimental set up for inducing the transformations on quasi-percolated Ag thin films deposited on TEM grids. Typical distances are d = 15 cm and D = 1 μm. A diffractive element (diff. ele.) can be introduced in the optical path as explained in the text.

3. Characterization of the samples

The as grown non-irradiated and irradiated silver nanostrucures were characterized by TEM and AFM microscopies. A Carl Zeiss model EM10 conventional TEM with 0.4 nm resolution at 120 kV was used to characterize the samples. This is a useful technique which gives two-dimensional information. In order to measure the height of the nanostructures AFM microscopy was performed. The AFM analysis, was done in Nanoscope III, Digital Instruments, USA. The instrument was operating in the 'tapping' mode, in air, following a rather standard procedure. Special attention was given to minimize the force between the AFM tip and the sample surface, due to the possibility of damaging the amorphous carbon and Al_2O_3 films of the TEM grid on which silver nanoparticles were deposited. Due to the same reason, images were recorded at a very slow scan rate: below 1 Hz. In order to place the AFM tip always on the same spot (within 10 μm), before and after treatment with UV laser, an optical microscope (mag. 400X) was used. This is also of great help in order to choose a reasonably flat quadrant (figure 2).

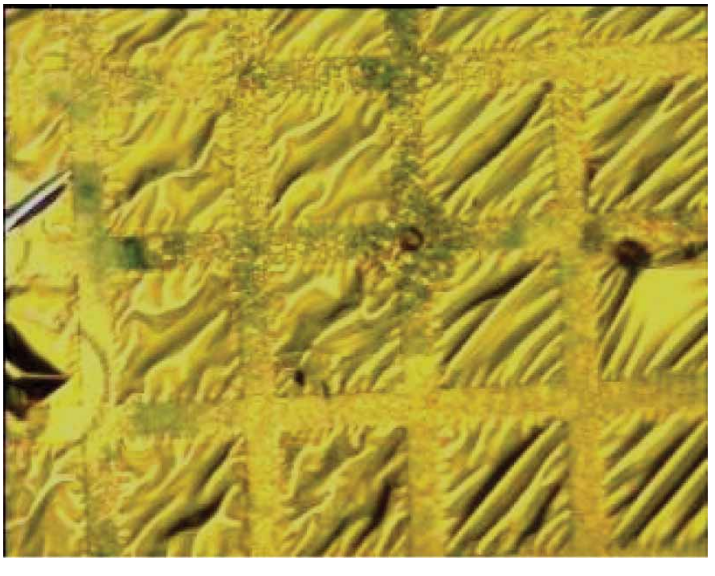

Figure 2. Optical image of the TEM copper 200 mesh square grid, with silver nanoparticles deposited on the top of the thin amorphous carbon/Al_2O_3 film. Image was recorded just after PLD process, before being subjected to the UV laser irradiation treatment. Image size: 540 μm × 400 μm.

It is worth mentioning the advantage in depositing on the TEM microscopy grid, which was crucial during the identification of the same imaging area. The TEM grid has a mark at the center of the sample which helps significantly in identifying quadrant orientations as shown in figure 2. Images were recorded in the height (topography), amplitude and phase mode simultaneously. However, for the purpose of particle size analysis, only the height mode images were taken into account. Quantitative evaluations including the surface roughness (RMS), were performed using the NanoScope-associated software.

4. Results and discussion

4.1 *Size and shape changes as a function of the number of pulses and the energy density. TEM characterization.*

The laser irradiation of nanoparticles induces changes in their size and shape [1, 17]. We have irradiated a sample which is in a quasi-percolated state as shown in figure 3. From previous results it is important to note that the observed changes take place upon irradiation in a relatively small range of energy densities; from 20 to 30 mJ/cm^2. Below the minimum value no modifications are detected on the sample and above the maximum value strong damage occurs [11]. We have found a precise irradiation energy, which induces the transformation of the quasi-percolated pattern into individual spherical shaped nanoparticles [11]. This phenomenon can be explained because heating will allow the nanostructures to reshape into their most thermodynamically stable shape, that of a solid truncated sphere. The effect of the irradiation is to increase the size of the nanoparticles keeping their spherical shape as shown in figure 4 (a–c). One observes that the size of the spherical nanoparticle increases with the number of pulses. The mean size of the nanoparticles starts at 38 nm for the first pulse (figure 4a), for

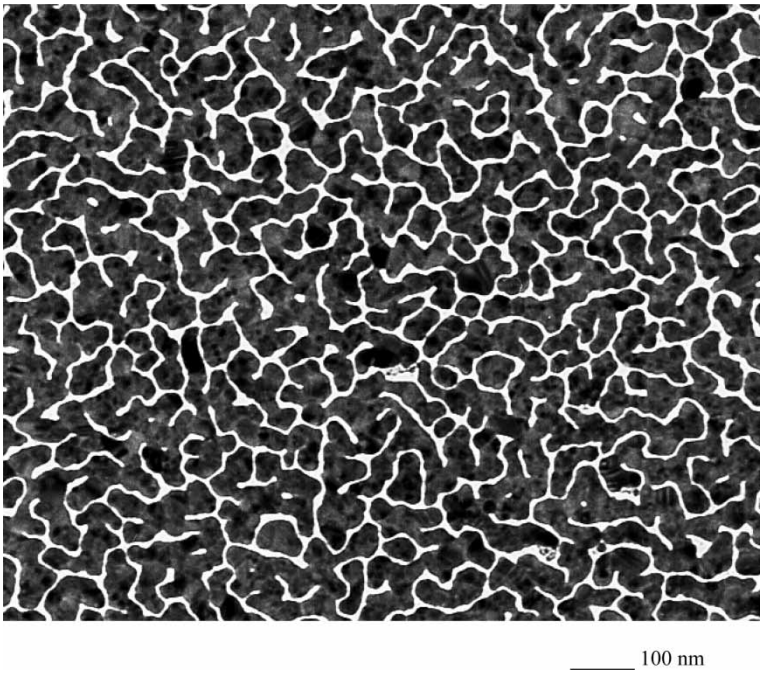

Figure 3. TEM photograph of the quasi-percolated Ag film.

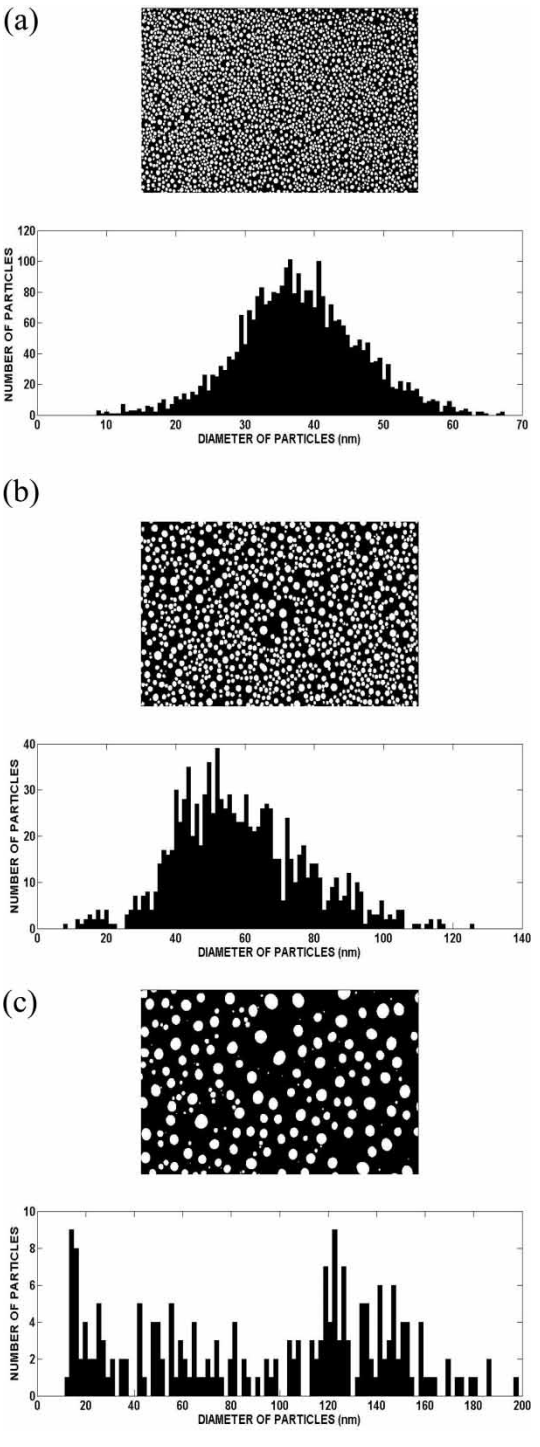

Figure 4. Treated images of the TEM photographs with their corresponding size distributions. 4a, 4b and 4c after 1, 2 and 3 laser pulses respectively.

the second pulse this value increases to 52 nm (figure 4b) and finally reaches 120 nm for the third pulse (figure 4c). The most probable mechanism responsible for this increase in size is Ostwald ripening [18]. Preliminary results tend to indicate that upon further irradiation the increase is less important implying that the particles reach an equilibrium size. This was reported before for gold nanoparticles supported in SiO_2/Si surface [10]. Recently a simple model has been suggested for the maximum particle diameter in the case of gold nanoparticles in an aqueous solution. According to this model the maximum particle diameter is controlled by the competition between heating by the laser beam and heat dissipation from the particle surface to the surroundings [19]. In the present case, the energy absorption is likely to occur in the silver nanostructures resulting in their melt and subsequent cooling adopting a spherical shape [11].

4.2 *Size and shape changes as a function of the number of pulses and the energy density. AFM characterization.*

The main reason to take AFM images of the particular samples was to evaluate the size of the silver nanoparticles as three-dimensional objects in comparison to TEM analysis which gives two-dimensional information. As one can see both techniques have a very high-spatial resolution and detection of nanoparticles with diameters of a few tenths of nanometer is not difficult. Furthermore, the shape of silver nanoparticles appears to be identical in images obtained by both microscopy techniques: TEM and AFM.

The AFM images of the silver nanoparticle film were taken before and after the UV laser treatment. Figure 5a shows a typical high-resolution AFM image of the non-irradiated silver film. The structure is very similar to the one obtained by TEM i.e. a quasi-percolated silver film. The image surface was 642 nm $\times$ 642 nm, equivalent to an area of 4.12×10^5 nm^2. The surface was found to be covered by the fingered shaped aggregates of silver nanoparticles. In this particular image, one can identify 27 aggregates, which are formed by 102 individual spherical silver nanoparticles. These aggregates of nanoparticles have different diameters. They can be divided mainly into two groups: first, particles with diameter of 21 ± 1 nm (about 70% of the total number of nanoparticles) and bigger ones with diameter of 30 ± 1 nm. However these two groups differ significantly in their height. The smaller ones have a height of only 7 ± 0.5 nm, and the height of the larger structures is 14 ± 1 nm. The (RMS)/Rq factor, as the measure of roughness, of the imaged surface is 2.07 nm.

Figure 5b, shows practically the same area of the sample surface after the UV laser irradiation treatment of the quasi-percolated silver nanoparticles film. The morphology of the silver PLD film has completely changed. AFM images reveal a rather small number (43) of individual oblate nanoparticles, with diameters ranging from 33 ± 0.5 to 46 ± 1 nm, and heights ranging from 14 ± 1 to 24 ± 1 nm, respectively. A simple quantitative analysis (counting the nanoparticles on the image) shows almost equal distribution between particles of both diameters (50% : 50%). In comparison with the non-irradiated films, the silver particles observed here are bigger in diameter and in height. Note, that in both figures, AFM images are presented with the same z-scale (0–60 nm), for easier comparison. The (RMS)/Rq factor, for the film in figure 5b, is 6.80 nm, which shows that the surface roughness is more important than in figure 5a.

One fundamental question is if the material found in the silver aggregates (figure 5a), is totally transformed into isolated spherical nanoparticles as seen in figure 5b. To evaluate if part of the silver evaporates during the irradiation process more detailed measurements are under progress. Note, that AFM is able to characterize the sample morphology with atomic resolution, but exclusively the top-surface layer. Existence of one or two monolayers beneath

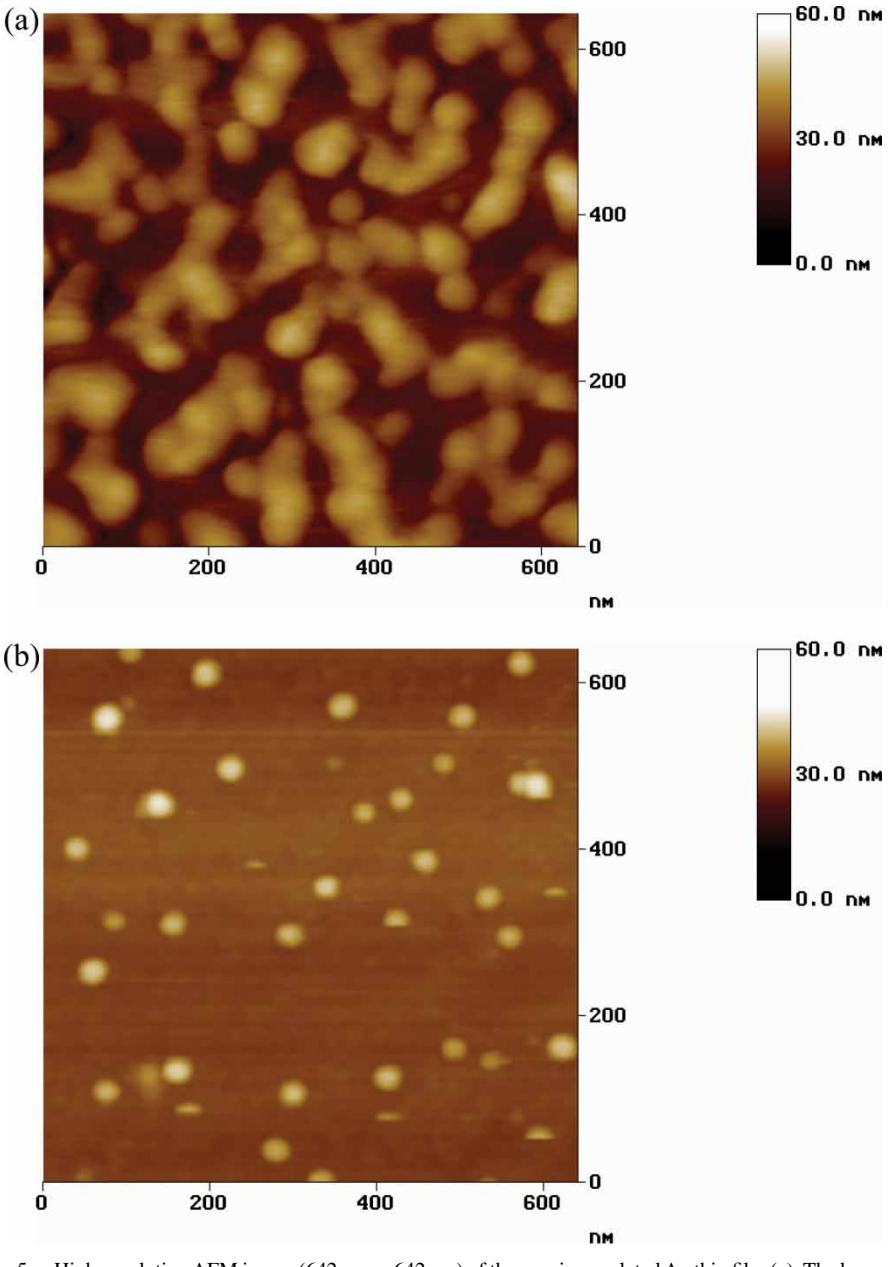

Figure 5. High-resolution AFM image (642 nm × 642 nm) of the quasi-percolated Ag thin film (a). The bean shape nanostructures are aggregates of the individual silver nanoparticles of different diameters: 21 and 30 nm, and height: 7 and 14 nm, respectively. High-resolution AFM image of the silver PLD film after UV 1 laser pulse (b). The image reveals individual spherical shaped nanoparticles of silver, with diameter in the range of 33–46 nm, and height of 14–24 nm.

the top adlayer will not change sample topography. On other side, TEM images shows all particles in the sample, including bulk and top layer, regardless to their position towards the surface. Due to this fact, TEM could be less sensitive in detection of the top surface monolayers. Conclusive results cannot be drawn at the present moment further experiments are currently under progress in order to further investigate these particular points.

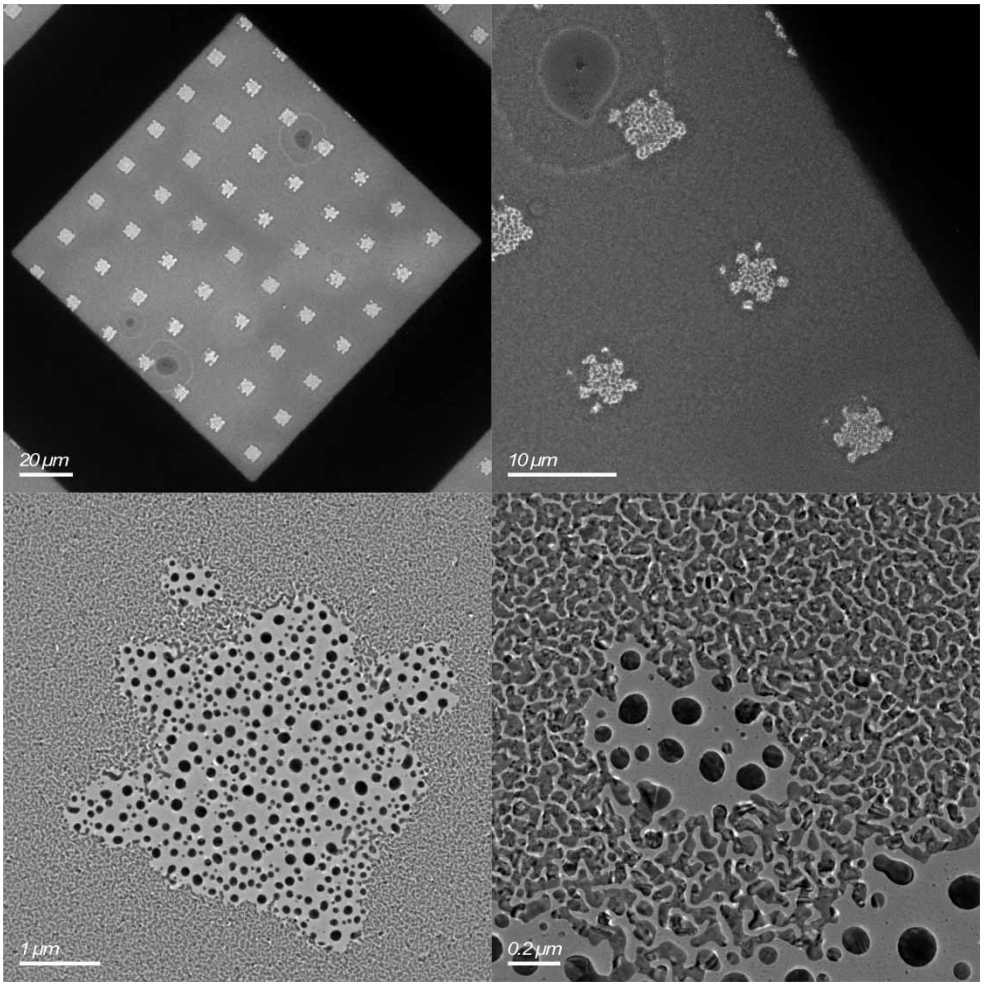

Figure 6. TEM image of the quasi percolated Ag thin film after 1 pulse laser irradiation through a 2000 mesh TEM grid.

The organization of nanoparticles under pulsed laser irradiation can be viewed as a structured light field that induces selectively a nucleation-growth process in the material. This patterning of the light field can be easily achieved by using different types of obstacles [10, 11, 20, 21]. The diffractive properties of these obstacles, that can have different geometries, are expected to modulate the intensity of the laser light at the surface of the sample therefore inducing changes in the nanostructures shapes and configurations.

The effect of introducing a diffractive element in the laser path and just before the quasi-percolated silver thin film is shown in figure 6. The diffractive element is simply a TEM grid (2000 mesh) and is placed in the laser optical path as shown in figure 1. The diffraction pattern imprinted in the film after irradiation through this particular mask corresponds to a square aperture [11, 21]. Magnification of the images show that the nanoparticles formed in the high-intensity regions of the diffraction pattern have sizes of the order of 50 nm. As shown before this technique allows to pattern the film similarly to other lithographic techniques.

5. Conclusions

The AFM and TEM analysis offer very useful data in the process of characterization of the silver nanoparticles. Indeed, very good agreement was achieved in terms of particle size, for both techniques. In addition, AFM images revealed valuable information about the nanoparticle height. It clearly shows how these two techniques can be used as complementary tools. The laser-induced patterning on the quasi-percolated film is an accurate imprint of the structured light field intensity obtained by introducing a square TEM grid. Different morphologies separated only by a few tenths of nanometer are clearly distinguishable. This 'lithographic' technique could be applied in high-resolution patterning.

References

[1] M. Vollmer, R. Weidenauer, W. Hoheisel, U. Schulte, F. Träger, Phys. Rev. **B40**, 12509 (1989).
[2] S. Ito, T. Mizuno, H. Yoshikawa, H. Masuhara, Jpn. J. Appl. Phys. **46** L241 (2007).
[3] A. Takami, H. Yamada, K. Nakano, S. Loda, Jpn. J. Appl. Phys. **35** L781 (1996).
[4] F. Mafune, J.Y. Kohno, Y. Tkeda, T. Kondow, J. Phys. Chem. B **105** 9050 (2001).
[5] S. Link, C. Burda, M.B. Mohamed, B. Nikoobakht, M.A. El-Sayed, J. Phys. Chem. B **103** 1165 (1999).
[6] M. Kaempfe, T. Rainer, K.J. Berg, G. Seifert, H. Graener, J. Phys. Chem. B **104** 11874 (2000).
[7] H. Kurita, A. Takami, S. Koda, Appl. Phys. Lett. **72** 789 (1998).
[8] M. Sugiyama, S. Inasawa, S. Koda, T. Hirose, T. Yonekawa, T. Omatsu, A. Takami, Appl. Phys. Lett. **79** 1528 (2001).
[9] J. Bosbach, D. Martin, F. Stietz, T. Wenzel, F. Träger, Appl. Phys. Lett. **74** 2605 (1999).
[10] M. Yang, M. Meunier, E. Sacher, J. Appl. Phys. **95** 5023 (2004).
[11] E. Haro-Poniatowski, J.P. Lacharme, E. Fort, C. Ricolleau, Appl. Phys. Lett. **87** 143103 (2005).
[12] I. Romero, J. Aizpurua, G.W. Bryant, F.J. García de Abajo, Opt. Express **14** 9988 (2006).
[13] J.J. Mock, M. Barbic, D.R. Smith, D.A. Schultz, S. Schultz, J. Chem. Phys. **116** 6755 (2002).
[14] P. Etchegoin, R.C. Maher, L.F. Cohen, H. Hartigan, R.J.C. Brown, M.J.T. Milton, J.C. Gallop, Chem. Phys. Lett. **375** 84 (2003).
[15] A.J. Haes, C.L. Haynes, A.D. McFarland, G.C. Schatz, R.P. Van Duyne, S. Zou, Mat. Res. Bull. **30** 368 (2005).
[16] M.J. Kaempfe, H. Graener, A. Kiesow, A. Heilmann, Appl. Phys. Lett. **79** 1876 (2001).
[17] F. Stietz, Appl. Phys. **A72** 381 (2001).
[18] I.M. Lifshitz, V.V. Slyozov, Soviet Phys. JETP **35** 331 (1959).
[19] S. Inasawa, M. Sugiyama, S. Koda, Jpn. J. Appl. Phys. **42** 6705 (2003).
[20] M. Fernández-Guasti, M. de la Cruz Heredia, J. Mod. Opt. **40** 1073 (1993).
[21] R. Riedel, J.L. Hernández-Pozos, R.E. Palmer, K.W. Kolasinski, Appl. Phys. **A78** 381 (2004).